Trans Indian Inst Met (2015) 68(4):581–586
DOI 10.1007/s12666-014-0487-3

TECHNICAL PAPER

TP 2882

Dry Sliding Wear Properties of HVOF Sprayed WC–10Co–4Cr Coating

Yuping Wu · Bo Wang · Sheng Hong · Jianfeng Zhang · Yujiao Qin · Gaiye Li

Received: 21 September 2013 / Accepted: 11 November 2014 / Published online: 30 December 2014

Abstract The high-velocity oxygen-fuel (HVOF) spraying process was used to prepare WC–10Co–4Cr coating onto AISI 1045 steel substrate. The microstructure, hardness and dry sliding wear behavior of the coating were investigated and compared with cold work die steel Cr12MoV. The results showed that, the coating had low porosity, high microhardness, and homogeneous distribution of WC particles. The coating was composed of WC and W_2C phases. With increase in load, the friction coefficients of the coating and the cold work die steel Cr12MoV decreased. The friction coefficients and wear mass losses of the coating were lower than that of the steel Cr12MoV. The dominant wear mechanism of the coating under both loads (30 and 50 N) was extrusion deformation and abrasion wear. For steel Cr12MoV, the dominant wear mechanism was plastic deformation and oxidation.

Keywords WC–10Co–4Cr · HVOF · Wear · Coating

1 Introduction

Die steels play an important role in many industries because of their advantages such as high use ratio of materials, low finish allowance and short process time [1]. However, the operation life of die steels has been decreased by their lower wear resistances. WC–Co based coatings are commonly used to improve the wear resistance of engineering components, which is due to the advantageous combination of hardness and toughness [2, 3]. High velocity oxygen fuel (HVOF) spraying has been proved to be one of the best thermal spraying techniques to deposit WC–Co based feedstock powders [4]. The reason is that the WC powder particles have less probability of decomposition during the HVOF spraying process than that of many other thermal spraying methods [5]. Moreover, HVOF sprayed WC–Co based coatings exhibits lower porosity, high hardness and bonding strength, which is beneficial for the wear resistance [6, 7]. Some literatures have reported that morphology of the feedstock powders, type of HVOF spray system and spray parameters would affect the microstructure and, in turn, the wear resistance of the as-sprayed coatings [8, 9].

Many investigations have been conducted on the wear performance and mechanism of HVOF sprayed WC–Co based coating. Żórawski [10] compared the abrasive wear resistances of HVOF sprayed nanostructured and conventional WC–12Co coatings. They showed that the nanostructured WC–12Co coating had denser structure, higher hardness and abrasive wear resistance than the conventional coating. Hazra et al. [11] founded that the HVOF sprayed WC–12Co coating had higher wear resistance than that of the plasma sprayed WC–12Co coating and the hard chromium coating, which is attributed to its higher hardness and less porosity. Saha and Khan [12] demonstrated that the HVOF sprayed near-nanocrystalline WC–17Co coating had superior wear resistance compared with HVOF sprayed microcrystalline WC–10Co–4Cr coating. The effects of the mixing of powders with various particle sizes on the fracture toughness and wear resistance of HVOF sprayed WC–10Co–4Cr coating were investigated by Lee et al. [13]. Staia and Carrasquero [14] studied the tribological properties of HVOF sprayed WC–14Co–3Cr

Present Address:
Y. Wu (✉) · B. Wang · S. Hong · J. Zhang · Y. Qin · G. Li
Institute of Metals and Protection, College of Mechanics and Materials, Hohai University, 1 Xikang Road, Nanjing 210098, Jiangsu, People's Republic of China
e-mail: wuyuping@hhu.edu.cn; wuyphhu@163.com

coating and concluded that the wear mechanism for the coating was a mixed wear mechanism of both abrasive and adhesive wear.

In our early work, a detailed characterization on the microstructures and thermostability of HVOF sprayed WC–10Co–4Cr coating was conducted [15]. In the present work, the coating was characterized based on microstructures and physical properties and further evaluated for its dry sliding wear behavior and mechanism under different loads. Wear property and mechanism of the coating was compared with the cold work die steel Cr12MoV.

2 Experimental Procedure

The powder used for this work was a commercial agglomerated and sintered WC-10 wt% Co-4 wt% Cr powder (Large Solar Thermal Spraying Material Co. Ltd, Chengdu, China), which had particle size distribution between 15 and 45 μm. The substrate of the coating was AISI 1045 steel. Before the HVOF spraying process, all the substrates were degreased with acetone, dried by hot air, and then grit-blasted with 30 meshes Al_2O_3. Then a commercial spray gun (Praxair Tafa-JP8000, USA) was used to deposit WC–10Co–4Cr coating on the substrate. The optimum parameters of the spraying process were listed in Table 1.

In order to identify the phases composition, X-ray diffraction (XRD, Bruker D8-Advanced, Germany) was performed on the as-sprayed coatings with Cu Kα radiation and step 0.02°. Microstructures of the as-sprayed coating and the worn surfaces were studied using a scanning electron microscope (SEM, Hitachi S-3400N, Japan) and an environmental scanning electron microscope (ESEM, Philips XL30, Holland) equipped with an energy dispersive X-ray (EDX, FEI Genesis 60S, Holland) analysis system. The porosity of the coating was determined by using an optical microscopy (OM, OLYMPUS BX51 M, Japan) fitted with an image analyzer, on polished cross sections of the coating at a magnification of 500× . Microhardness measurements were performed on the transverse section of the coating under a load of 1.96 N for 15 s using a Vickers microhardness tester (HXD-1000TC). Twenty porosity and hardness measurements were taken of the coating section and averaged to ensure the data repeatability.

Table 1 Parameters of HVOF spraying process

Spray parameters	Value
Kerosene flow rate (L min^{-1})	0.38
Oxygen flow rate (L min^{-1})	897
Spray distance (mm)	300
Carrier gas flow rate (L min^{-1})	10.86
Powder feed rate (rpm)	5
Spray gun speed (mm s^{-1})	280

The dry sliding wear tests were conducted on a MG-2000 pin-on-disk tribometer (Beilun Balancing Machinery Co. Ltd., Zhangjiakou, China). The test was performed in accordance with the standard ASTM G99-05 [16]. The wear specimens (Φ45 mm × 7 mm) of HVOF sprayed WC-10Co-4Cr coating and the cold work die steel Cr12MoV were rotated during the test. The upper pin of Al_2O_3 ball (Φ6 mm) was stationary. The wear test was performed under the following conditions: sliding velocity of 0.9 m s^{-1}, sliding distance of 1,500 m, normal loads of 30 and 50 N. The ambient temperature and the relative humidity varied between 20 and 25 °C and between 40 and 50 %, respectively. Prior to the wear test, the surface of all specimens was ground and polished to a mirror-like surface with an average surface roughness $R_a = 0.12$ μm, degreased in acetone in an ultrasonic bath and dried in warm air. The wear mass loss of the specimens was determined by using an analytical balance with an accuracy of 0.1 mg before and after the test. The frictional moments were recorded by a computer consistently. The worn surface morphologies were observed by OM and SEM.

3 Results and Discussion

3.1 Characterisations of the Coating

Figure 1 shows the XRD pattern for the surfaces of the HVOF sprayed WC-10Co-4Cr coating. It can be seen that the coating is mainly composed of WC (JCPDS 89-2727) and W_2C (JCPDS 35-776) phases. The slight shift between the observed peak of W_2C and the nominal position (based on JCPDS 35-776) may be explained by a slight doping with Cr, which causes a change in lattice parameters [17].

Figure 2 illustrates a typical region from the polished cross-sections of the coating. It can be seen from Fig. 2a that the coating is very dense, smooth, and without cracks. Some alumina grits maybe trapped in coating/substrate interface region. The thickness of the coating is around 200 μm. Figure 2b shows a detailed microstructure of the coating, where a much larger volume fraction of tungsten carbides are uniformly distributed in the coating. Some pores are visible as very dark regions in the coating. The average porosity of the coating was determined to be 0.51 % by image analysis. A similar morphology has been observed in previous investigations [15, 18–20].

The microhardness of the coating with respect to the distance to the coating-substrate interface is shown in Fig. 3. It can be seen that the microhardness of the coating is in the range of 1168–1323 HV_{200}. The non-uniformity of

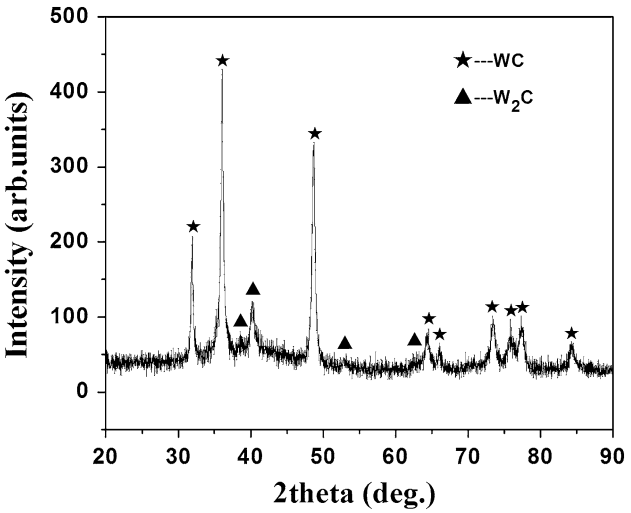

Fig. 1 XRD pattern of the WC-10Co-4Cr coating

the microhardness is attributed to the inhomogeneous distribution of the porosity. The average microhardness value of the coating is 1233 ± 64 HV_{200}, which is much higher than that of the substrate (230 ± 17 HV_{200}). This is thought to be affected by the low porosity and the presence of hard phases (i.e. tungsten carbide) shown in Figs. 1 and 2.

3.2 Characteristics of Wear

Figure 4 shows the friction coefficients of the WC–10Co–4Cr coating and the cold work die steel Cr12MoV. It is seen that the friction coefficients of the coating and steel Cr12MoV both have a "run-in" period. A similar phenomenon was observed by other researchers [2]. The friction coefficients of the coating and steel Cr12MoV are stable after 5 min of the wear testing. The friction coefficient of the WC–10Co–4Cr coating is lower than that of steel Cr12MoV under the stable period. The average friction coefficient of WC–10Co–4Cr coating decreases from approximately 0.50 to 0.47 when the load increases from 30 to 50 N. With the increase of load, the average friction coefficient of steel Cr12MoV decreases from 1.03 to 0.85. This is related to the actual contact area between the specimens and the counterpart during friction process. In this study, the interface heating increases with increasing normal load, which would increase the flow ability of ductile Co–Cr matrix. Thus greater extent of mechanically mixed layer and surface smoothening could be formed at higher normal load, which lead to the increment of the actual contact area and the reduction in friction coefficient [21, 22].

The wear cumulative mass loss curves of the WC–10Co–4Cr coating and the cold work die steel Cr12MoV are shown in Fig. 5. The result shows that the mass loss of the coating is significantly less than that of the steel

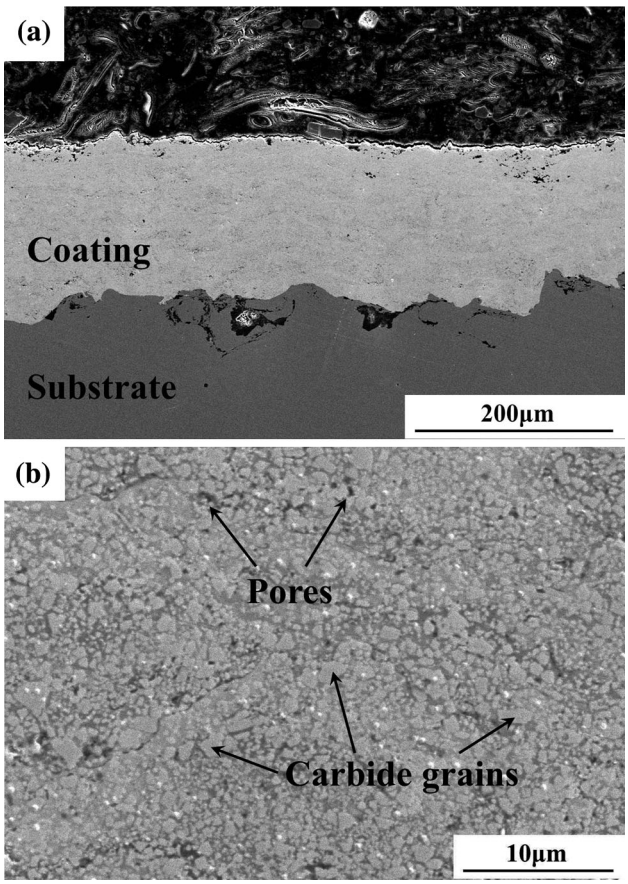

Fig. 2 SEM images of a transverse section of the WC-10Co-4Cr coating: **a** an overall view morphology, **b** pores

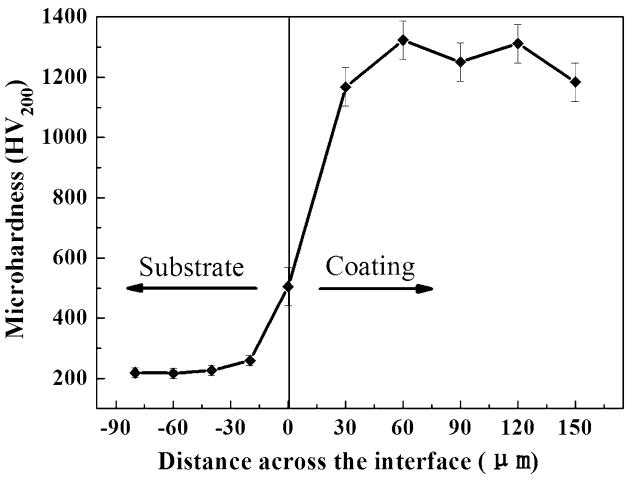

Fig. 3 Variation in microhardness across the WC-10Co-4Cr coating and substrate

Cr12MoV at the same wear conditions. The mass loss of the steel Cr12MoV is about 2.5 times and 3.5 times higher than that of the coating under loads of 30 N and 50 N, respectively. This indicates that the wear resistance of the coating is significantly improved compared with the steel

Cr12MoV. It is reported that a soft binder combined with a homogeneous dispersion of fine WC grains is beneficial for the wear resistance of the coating [2].

In order to understand the wear behavior, the worn scars were examined by SEM. Figure 6 shows the representative SEM images of worn morphology for the WC–10Co–4Cr coating against Al_2O_3 ball at room temperature under loads of 30 and 50 N. As shown in Fig. 6a, c, plowing traces, spalling, extrusion deformation and cracks are formed on the wear surface of the coating and the number of the plowing traces and cracks increases as the load increases. This indicates that the coating suffers serious wear damage during higher load. In addition, some carbide particles pullout appears in discrete areas, which is attributed to the cutting of two body abrasion particles on the surface of the coating [23]. Figure 6b, d shows higher magnification micrographs indicating that the wear of the coating is progressed by two possibilities: Due to squeezing action between the coating and alumina, extrusion deformation of soft metallic binder matrix form some flakes on the wear surface (region A); Cracks form on the surface due to the action of continuing stress (region B). A similar morphology has been observed before [24, 25]. As seen in Fig. 6d, the cracks around the pores are perpendicular to the sliding direction and propagate along the near pores. The dominant wear mechanism of the coating is extrusion deformation and abrasion wear.

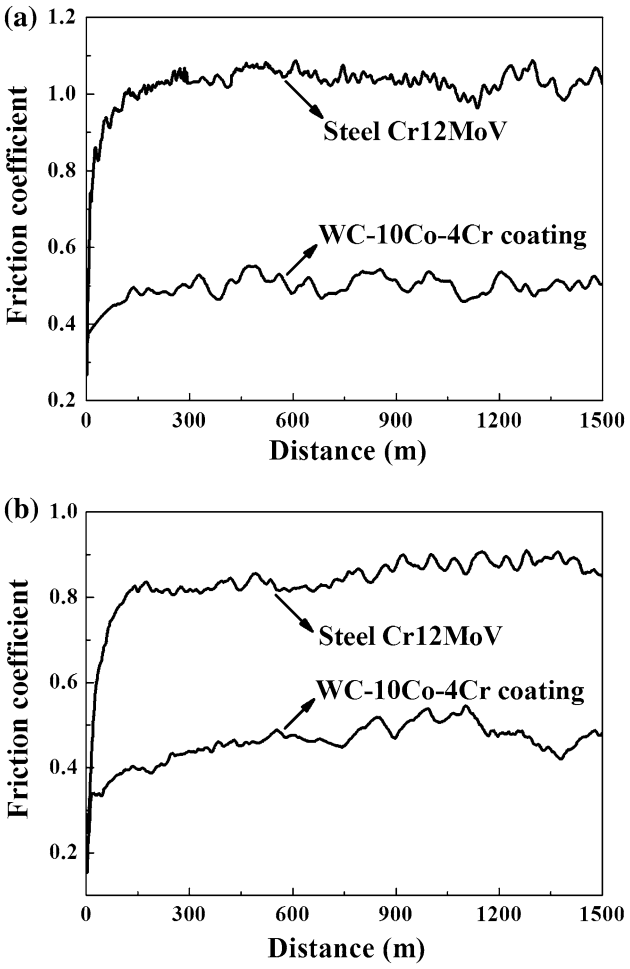

Fig. 4 Friction coefficients of the WC-10Co-4Cr coating and the cold work die steel Cr12MoV: **a** load 30 N, **b** load 50 N

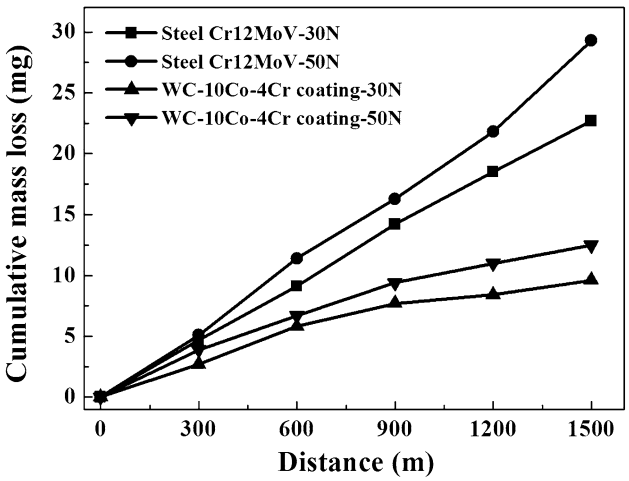

Fig. 5 Cumulative mass losses of the WC-10Co-4Cr coating and the cold work die steel Cr12MoV

OM and ESEM investigations of the worn morphology of the cold work die steel Cr12MoV under loads of 30 N and 50 N are shown in Fig. 7. From Fig. 7a, c, it can be noticed that there are grooves formed by plastic deformation and some partially oxidized tracks on the wear surface under a load of 30 N. The dark grey structure (point A) is confirmed to be iron oxide by the EDX analysis, as shown in Fig. 7d. The quantitative analysis (at%) is also given in Fig. 7d. Figure 7b shows that an oxide layer appears continuously and the grooves become deeper under a load of 50 N compared with that under a load of 30 N. This is the reason that the friction coefficient decreases as the load increases, as seen in Fig. 4. This phenomenon was similar to the results reported by other researchers [26–28]. It is supposed that the dominant wear mechanism of the steel Cr12MoV is plastic deformation and oxidation.

4 Conclusion

WC–10Co–4Cr coatings were fabricated by the HVOF spraying process. The coating had low porosity, high microhardness, and homogeneous distribution of WC particles. The friction coefficients of the WC–10Co–4Cr coating and the cold work die steel Cr12MoV were found to decrease progressively with the increase in load. The friction coefficients and wear mass losses of the coating were obviously lower than that of the steel Cr12MoV. The

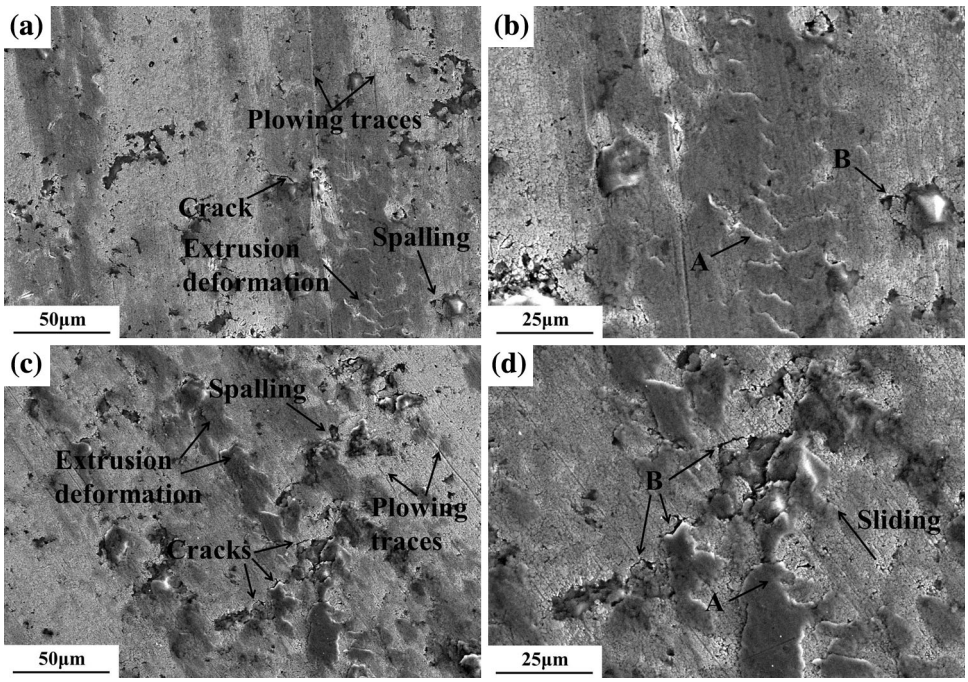

Fig. 6 Representative SEM images of wear-track morphology for the WC-10Co-4Cr coating: **a**, **b** load 30 N, **c**, **d** load 50 N

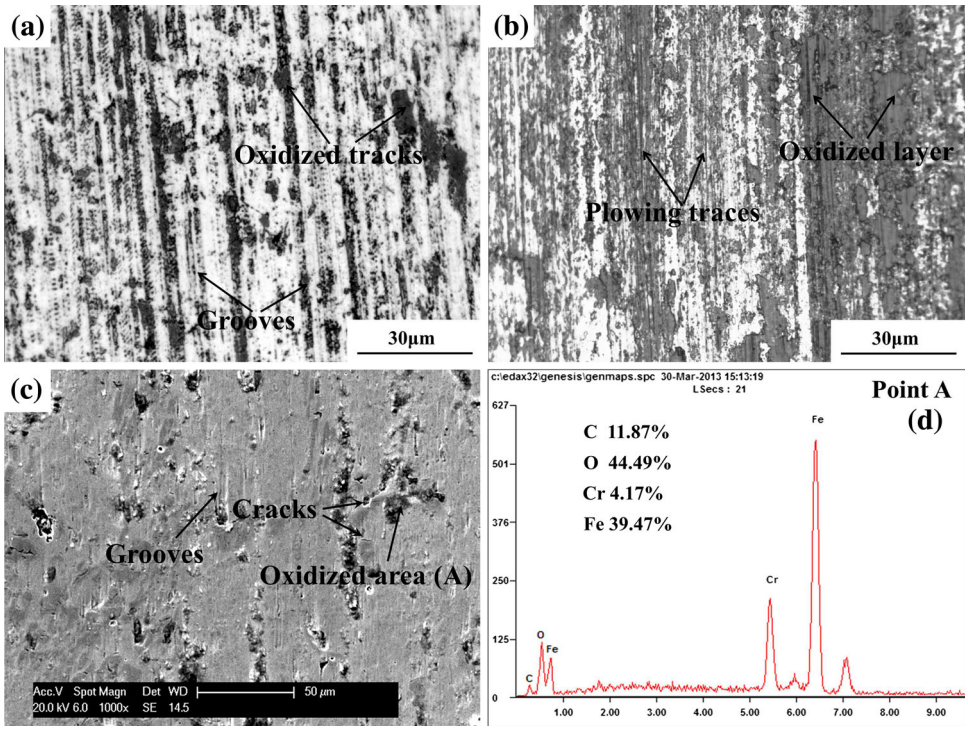

Fig. 7 Representative wear-track morphology for the cold work die steel Cr12MoV: **a** OM image of load 30 N, **b** OM image of load 50 N, **c** ESEM image of load 30 N, **d** EDX result of point A in (**c**)

dominant wear mechanism of the coating under both loads (30 and 50 N) was extrusion deformation and abrasion wear. For steel Cr12MoV, the dominant wear mechanism was plastic deformation and oxidation.

Acknowledgments The research was supported by the Fundamental Research Funds for the Central Universities (Grant nos. 2013B34414 and 2014B02314) and the Research and Innovation Project for College Graduates of Jiangsu Province (Grant no. CXLX12_0244).

References

1. Wei M X, Wang S Q, Zhao Y T, Chen K M, and Cui X H, *Metall Mater Trans A* **42A** (2011) 1646.
2. Zhu Y C, Yukimura K, Ding C X, and Zhang P Y, *Thin Solid Films* **388** (2001) 277.
3. Ghadami F, Ghadami S, and Abdollah-Pour H, *Vacuum* **94** (2013) 64.
4. Yoganandh J, Natarajan S, and Kumaresh Babu S P, *Trans Ind Inst Met* **66** (2013) 437.

5. Santana Y Y, La Barbera-Sosa J G, Caro J, Puchi-Cabrera E S, and Staia M H, *Surf Eng* **24** (2008) 378.
6. Santana Y Y, La Barbera-Sosa J G, Bencomo A, Lesage J, Chicot D, Bemporad E, Puchi-Cabrera E S, and Staia M H, *Surf Eng* **28** (2012) 237.
7. Thakur L, and Arora N, *J Mater Eng Perform* **22** (2013) 574.
8. Wang Q, Chen Z H, Li L X, and Yang G B, *Surf Coat Technol* **206** (2012) 2233.
9. Yin B, Zhou H D, Yi D L, Chen J M, and Yan F Y, *Surf Eng* **26** (2010) 469.
10. Żórawski W, *Surf Coat Technol* **220** (2013) 276.
11. Hazra S, Sabiruddin K, and Bandyopadhyay P P, *Surf Eng* **28** (2012) 37.
12. Saha G C, and Khan T I, *Metall Mater Trans A* **41A** (2010) 3000.
13. Lee C W, Han J H, Yoon J, Shin M C, and Kwun S I, *Surf Coat Technol* **204** (2010) 2223.
14. Staia M H, and Carrasquero E, *Surf Eng* **16** (2000) 515.
15. Hong S, Wu Y P, Gao W W, Wang B, Guo W M, and Lin J R, *Surf Eng* **30** (2014) 53.
16. ASTM G99-05 (2010), *Standard test method for wear testing with a pin-on-disk apparatus*, ASTM International, New york (2010).
17. Berger L, Saaro S, Naumann T, Kasparova M, and Zahalka F, *J Therm Spray Technol* **17** (2008) 395.
18. Hong S, Wu Y P, Li G Y, Wang B, Gao W W, and Ying G B, *J Alloy Compd* **581** (2013) 398.
19. Hong S, Wu Y P, Wang Q, Ying G B, Li G Y, Gao W W, Wang B, and Guo W M, *Surf Coat Technol* **225** (2013) 85.
20. Hong S, Wu Y P, Wang B, Zheng Y G, Gao W W, and Li G Y, *Mater Des* **55** (2014) 286.
21. Rajinikanth V, and Venkateswarlu K, *Tribol Int* **44** (2011) 1711.
22. Du H, Sun C, Hua W G, Wang T G, Gong J, Jiang X, and Lee S W, *Mater Sci Eng A* **445-446** (2007) 122.
23. Shipway P H, and Howell L, *Wear* **258** (2005) 303.
24. Heydarzadeh Sohi M, and Ghadami F, *Tribol Int* **43** (2010) 882.
25. Di Girolamo G, Marra F, Pulci G, Tirillo J, and Valente T, *Int J Appl Cerma Technol* **10** (2013) 60.
26. Varenberg M, Halperin G, and Etsion I, *Wear* **252** (2002) 902.
27. Li J L, Xiong D S, Zhang Y K, Zhu H G, Qin Y K, and Kong J, *Tribol Lett* **43** (2011) 221.
28. Li J L, Xiong D S, Wu H Y, Zhang Y K, and Qin Y K, *Surf Coat Technol* **228** (2013) S219.